Earthquake Geotechnical Engineering for Protection and Development of Environment and Constructions – Silvestri & Moraci (Eds)
© 2019 Associazione Geotecnica Italiana, Rome, Italy, ISBN 978-0-367-14328-2

Soil-foundation compliance effect on seismic vulnerability assessment of RC structures

C. Petridis & D. Pitilakis
Aristotle University of Thessaloniki, Thessaloniki, Greece

ABSTRACT: This paper presents an overview of soil-structure interaction effects on earthquake vulnerability assessment of reinforced concrete buildings. We examine (i) eighteen reinforced concrete building types, covering the structural typologies met in common engineering practice, (ii) seven soil profiles, representative of code-based soil classifications and (iii) three soil-foundation models, namely fixed-base, Beam-on-Nonlinear-Winkler elements and elastic springs. Eleven real earthquake recordings are used as input at bedrock level to obtain the corresponding free-field motions. Incremental Dynamic Analysis is applied to obtain a cloud of PGA - interstory drift pairs for all possible combinations. The corresponding fragility curves are derived and post-processed to estimate model-to-model differences within same structural typologies. The results are presented in heat map form, while an example in terms of loss curves is also given.

KEYWORD: SSI, fragility, nonlinear soil, vulnerability assessment

1 INTRODUCTION

Earthquakes represent a serious threat for many countries worldwide. Since the first studies on regional-scale seismic vulnerability assessment, during the early 1970s, the scientific state-of-the-art has undergone a notable development (Pitilakis et al. 2014). Over the years, various approaches have been adopted to model the structural typologies met in engineering practice, examining full models (Kappos et al. 2006), multi-degree-of-freedom or single-degree-of-freedom equivalent models (Pinho et al. 2002, Crowley et al. 2004). Furthermore, material aging effects (Pitilakis et al. 2013), site effects (Pitilakis & Petridis 2018), geotechnical hazards and epistemic uncertainties have been included in many studies, leading to a large number of ready-to-use fragility curves (Yepes-Estrada et al. 2016). A known yet unquantified issue is the influence of soil-structure interaction (SSI), as well as the nonlinear soil behavior effects that come along. Some studies have demonstrated that SSI may significantly alter the structural response in terms of earthquake vulnerability (Rajeev & Tesfamariam 2012, Pitilakis et al. 2013, Petridis & Pitilakis 2018), often leading to increased damage. However, large-scale risk assessment requires an efficient overview of the problem, rather than a building-specific approach. The purpose of this study is to investigate the influence of SSI on earthquake fragility and combine nonlinear soil behavior and SSI effects on seismic vulnerability. We focus on highlighting the differences that occur when SSI is included for a set of typical reinforced concrete (RC) buildings on different soil profiles, rather than providing case-specific fragility curves.

2 NUMERICAL MODELING

2.1 *Buildings examined*

We examine a set of eighteen typical reinforced concrete buildings with a view to covering the corresponding structural typologies met in common engineering practice (Kappos et al. 2006). In particular, the following configurations are considered:

– (i) dual (frame + shear wall) systems and (ii) moment resisting frames
– (i) low-rise (2-story), (ii) mid-rise (4-story) and (iii) high-rise (9-story) buildings
– (i) no infills (bare), (ii) regularly infilled and (iii) soft story (pilotis) systems

The 2D numerical models are developed in OpenSees (Mazzoni et al. 2009). In particular, the uniaxial "Concrete01" and "ReinforcingSteel" materials are used to create the fiber sections of each structural element modeled; "Concrete01" material object implements the modified Kent & Park concrete model (Kent & Park 1971) proposed by Scott et al. (1982) with degraded linear unloading/reloading stiffness based on the work of Karsan & Jirsa (1969); "ReinforcingSteel" implements the reinforcing steel material model, based on the backbone curve described by Chang & Mander (1994). The nonlinear RC behavior is thus inherently considered, adopting a distributed plasticity approach.

2.2 *Underlying soil profiles*

We select seven indicative soil profiles, ranging from rock to very soft clay. The characteristics of these profiles affect the stiffness and damping of the geotechnical part of the foundation, i.e. the foundation-soil system. A pseudo-1D equivalent of the physical free field is modeled, developing a column of two-dimensional "Quad" elements in OpenSees, for each soil type selected. Soil nonlinearities are inherently taken into account via the use of the "PressureIndependMultiYield" soil material. A single "zeroLength" element is used to define the Lysmer & Kuhlemeyer (1969) dashpot, demanding the input motion at the base of the soil column in velocity terms. The resulting force history is obtained by multiplying the known velocity time series by a constant factor set as the product of the area of the soil column base with the mass density and the shear wave velocity of the underlying bedrock. The mesh size is determined by the scheme of resolving the propagation of the shear waves at/below a specified frequency, ensuring that an adequate number of elements fit within the wavelength of the shear wave considered. This guarantees that the mesh is refined enough, so that the desired aspects of the propagating waves are fully captured during the dynamic analysis. Table 1 shows the suggested soil parameter values (OpenSees) and Table 2 presents the selected soil profiles.

2.3 *Soil-structure interaction*

Inertial soil-structure interaction effects are implemented using two different configurations: (i) Beam-on-Nonlinear-Winkler-Foundation (BNWF) spring-type elements (Raychowdhury 2008) and (ii) lumped individual elastic springs (LumpSpr) (Pais & Kausel 1988). Foundation depth is assumed equal to 2.0m, while a 0.0m foundation depth case is also examined. The corresponding fixed-base models are also implemented, highlighting the influence of SSI.

Table 1. Selected soil profiles and suggested parameter values (Mazzoni et al. 2009).

Parameters	Soft Clay	Medium Clay	Stiff Clay
Soil mass density	1.3 ton/m^3	1.5 ton/m^3	1.8 ton/m^3
Low-strain shear modulus	1.3x10^4 kPa	6.0x10^4 kPa	1.5x10^5 kPa
Bulk modulus	6.5x10^5 kPa	3.0x10^5 kPa	7.5x10^5 kPa
Cohesion	18 kPa	37 kPa	75 kPa
Shear strain at max shear	0.1	0.1	0.1
Friction angle	0.0	0.0	0.0

Table 2. Soil profiles examined.

No.	1	2	3	4	5	6	7
Vs (m/s)	>800	450	360	300	250	180	150
Type (EC8)	A	B	C	C	C	D	D

The BNWF model is developed using the ShallowFoundationGen OpenSees command. The footing model consists of a system of closely spaced independent nonlinear springs, coupled with a dashpot and gap elements, adopting the backbone curves of the nonlinear springs. Vertical springs distributed along the base of the footing aim to capture the rocking, uplift and settlement, whereas horizontal springs attached to the sides of the footing are used to capture the resistance against sliding and passive pressure. The BNWF model parameters have been calibrated against centrifuge experiments (Raychowdhury & Hutchinson 2009).

On the other hand, a set of three individual elastic springs for each footing is used in the second foundation formulation to simulate the horizontal, vertical and rotational stiffness, representing a rather oversimplified - but common - engineering practice.

Kinematic interaction effects in the Foundation Input Motion (FIM) are accounted using Mylonakis et al. (2006) equations for 2.0m foundation depth, while a 0.0m foundation depth case is also examined, neglecting kinematic interaction effects, where the input motion in the structure is the Free-Field Motion (FFM).

3 ANALYSES

3.1 *Earthquake recordings*

We select a set of eleven real earthquake recordings referring to eleven independent earthquake events, all of them recorded on sites classified as rock according to EC8. This number of records is considered adequate following the procedure described in the guidelines of Global Earthquake Model (GEM) for developing analytical seismic vulnerability functions (D'Ayala et al. 2013). These recordings were deliberately chosen to represent the ground motion at the underlying bedrock, eliminating any site effects and soil uncertainties. We intentionally exclude any duplicate events to derive a set of independent records. All the seismic events are characterized by a M_w>5.5 (Type 1 EC8 spectrum). This filtering procedure is rather exhausting for the existing strong motion databases, since only a limited number of such records is available. This procedure is followed by an iterative routine which attempts to match the EC8 target spectrum and further eliminates a number of records; consequently we end up with eleven ground motions presented in Table 3. Figure 1 shows the corresponding response spectra.

3.2 *Incremental dynamic analysis*

Incremental Dynamic Analysis (IDA) is performed to derive a cloud of intensity measure (IM) - engineering demand parameter (EDP) pairs (Vamvatsikos & Cornell 2002). We select PGA referring to the underlying bedrock as the IM and maximum interstory drift (maxISD) as the EDP. Qualifying PGA on rock conditions as IM facilitates highlighting the differences

Table 3. Selected earthquake recordings.

No.	Location	Database Code	R_{epi} (km)	M_w	PGA	$V_{s,30}$ (m/s)	Soil Type (EC8)
1	Tabas/Iran	ESMD_59	12.00	7.35	3.16	826.00	A
2	Montenegro/Montenegro	ISESD_223	21.00	6.90	1.77	1083.00	A
3	App.Lucano/Italy	ITACA_614	9.80	5.60	1.62	1024.00	A
4	Kobe/Japan	NGA_1108	25.40	6.90	2.85	1043.00	A
5	Sierra Madre/Mexico	NGA_1645	6.46	5.61	2.71	821.69	A
6	Loma Prieta/USA	NGA_3548	20.35	6.93	4.12	1070.34	A
7	Whittier Narrows/USA	NGA_680	13.85	5.99	1.10	969.07	A
8	Northridge/USA	NGA_994	25.42	6.69	2.84	1015.88	A
9	Izmit/Turkey	T-NSMP_1109	3.40	7.60	1.65	826.11	A
10	East Sicily/Italy	ITACA_314	28.30	5.60	0.61	871.00	A
11	Western Tottori/Japan	KIK-Net_3775	31.37	6.60	1.55	967.27	A

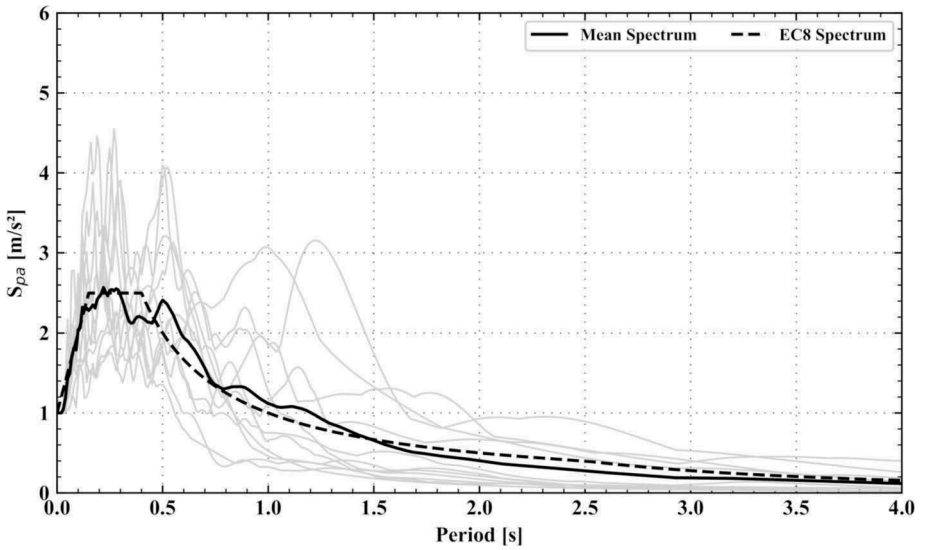

Figure 1. Normalized elastic response spectra of the selected ground motions; mean spectrum; EC8 spectrum.

introduced by soil nonlinearities; the use of maxISD as the EDP provides an efficient overview of the damage at global level, while the correspondence between maxISD and the moment-curvature diagrams at sectional level is also investigated with a view to relating maxISD to the actual structural damage of the structural elements. The ground motions selected are scaled from 0.0 to 1.0g in terms of the IDA performed, increased by a constant step of 0.05g.

3.3 *Fragility assessment*

Fragility curves represent the probability of exceeding a predefined limit state, as a function of an engineering demand parameter, under a seismic excitation of given intensity. Equation 1 describes the cumulative conditional probability of exceeding a DS for a given IM.

$$P[DS|IM] = \Phi\left(\frac{ln(IM) - ln(\overline{IM})}{\beta}\right) \tag{1}$$

Where Φ is the standard normal cumulative distribution function, IM is the intensity measure of the earthquake, $\overline{IM}$ is the corresponding median value, β is the log-standard deviation and DS is the damage state. In detail, the log-standard deviation parameter characterizes the total dispersion related to each fragility curve. Three primary sources of uncertainty which contribute to the total variability of any given limit state (NIBS 2004) are considered, namely (i) the variability related to the definition of the limit state value, (ii) the capacity of each structural model and (iii) the seismic demand. The log-standard deviation referring to the definition of the limit states is equal to 0.40, whereas the corresponding value regarding the capacity is assumed equal to 0.30 for no/low seismic code structural systems (NIBS 2004). The latter source of uncertainty, associated with the seismic demand, is explicitly evaluated, estimating the dispersion for the logarithms of PGA maxISD pairs, with respect to the regression method utilized.

Various DS definitions exist in literature, referring to different damage characteristics and threshold values. In order to disengage from the eternal selection procedure of the DS values, we focus on quantifying the differences between fixed and SSI-inclusive models, rather than presenting a set of case-specific fragility curves. Using Rossetto & Elnashai (2003) and Ghobarah (2004) drift-based DS limits as benchmark and slightly calibrating these values to approach the fixed-base fragility curves published by Kappos et al. (2006) for our identical

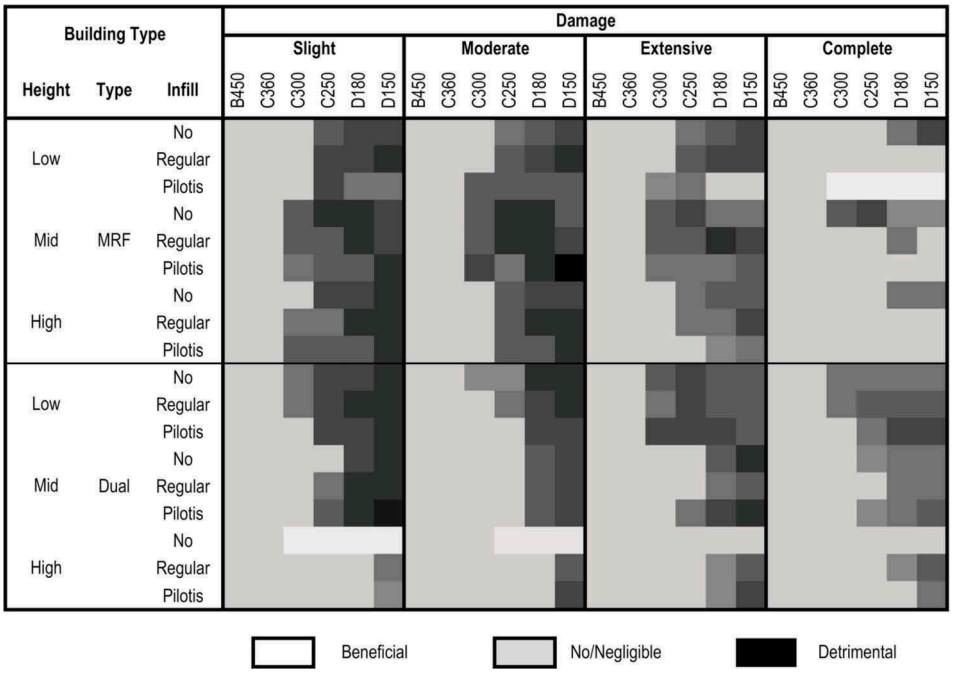

Figure 2. Ratios between the BNWF and fixed-base models in terms of PGA corresponding to 50% probability of exceeding a given DS.

fixed-base models, we obtain a set of DS values in terms of maxISD. Four DS are adopted, namely (i) SD: Slight damage, (ii) MD: Moderate damage, (iii) ED: Extensive damage and (iv) CD: Complete damage.

4 RESULTS

The results are presented measured in probability of exceeding different damage levels, using the fragility curves derived.

A general remark is that the influence of the nonlinear springs is higher than the one observed for the corresponding elastic springs. The use of the BNWF model is considered more elaborate and thus, the results presented herein compare BNWF to fixed-base models.

A second general remark is that SSI effects on fragility become significant only for soft soils, characterized by shear wave velocities less than around 300m/s. Again, any conclusions pointed out herein refer to soft subsoil conditions.

4.1 *Fragility*

A comprehensive set of fragility curves is derived for the buildings and soil profiles examined. For practical reasons, we investigate the model-to-model differences in terms of the PGA corresponding to 50% probability of exceeding a given DS, i.e. the median values. We calculate these ratios between the BNWF and fixed-base models and present them in Figure 2.

SSI influence becomes more apparent in lower DS. SD and MD levels are defined by low interstory drift limit values, thus they are sensitive to even slight changes introduced by SSI. In the case of infilled structures, SSI accelerates damage development by increasing the displacement demands imposed, which in turn is proven destructive for infill walls and early cancels their lateral stiffness; displacement-sensitive nonstructural elements, in general, presumably experience these damaging effects, however they are not addressed in this study.

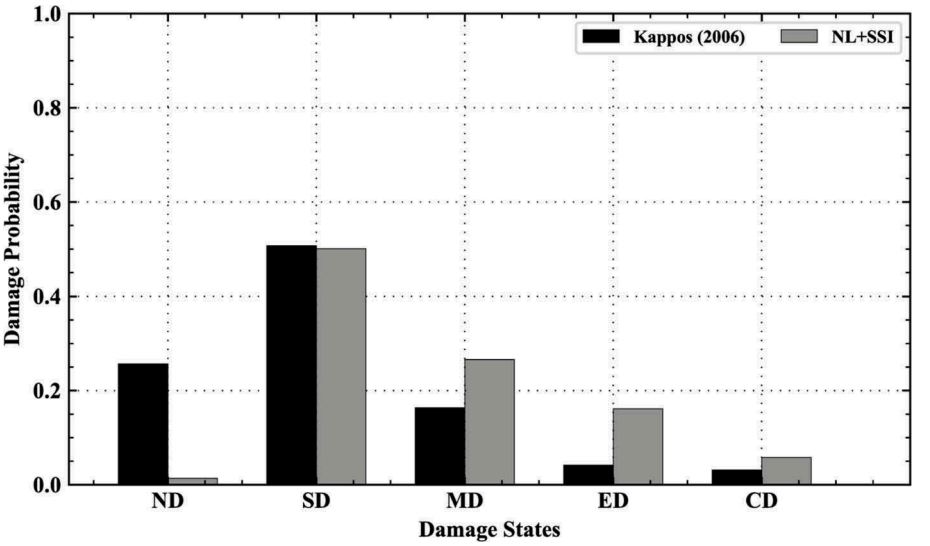

Figure 3. Damage probabilities for a (i) fixed-base on rock and (ii) flexible-base on soft clay (D180) 4-story dual, regularly infilled building, assuming a PGA=0.2g scenario.

For higher DS, SSI influences vulnerability in a different manner. In particular, for MRF structures SSI effects are either negligible or slight when the collapse/complete damage probability is assessed. On the contrary, SSI plays an important role when Dual systems are assessed. Specifically, a significant portion of the base reaction forces is transferred to the frame counterpart of the system, relieving shear walls, yet damaging the columns of the building.

4.2 *Vulnerability & losses*

Differences in terms of fragility influence the expected losses and the vulnerability of the structures. We select (i) Kappos et al. (2006) and (ii) Bal et al. (2008) damage indices to illustrate the corresponding losses.

Figure 3 presents the damage probabilities for a (i) fixed-base on rock and (ii) flexible-base on soft clay (D180) 4-story dual, regularly infilled building assuming a PGA=0.2g scenario.

Table 4 presents the corresponding damage factor, utilizing both indices. Nonlinear soil behavior and SSI nearly double the damage expected for the selected scenario.

Figure 4 shows the vulnerability/loss curves for these models, in the range of 0.0-10.0 m/s^2.

5 CONCLUSIONS

In this study, we investigated the influence of SSI on earthquake fragility curves for RC structures. SSI effects, as well as SSI and nonlinear subsoil behavior combined significantly alter the fragility of these structures for soft soil foundation conditions, detrimentally in most cases. While these effects may be captured in building-specific assessment, this study provides a general overview, useful for large-scale risk assessment. Furthermore, the results presented in heat map form may briefly guide insurers and catastrophe risk analysts.

ACKNOWLEDGEMENTS

We acknowledge support by the project "Innovative system for monitoring and early warning of schools and infrastructure against earthquakes and other hazards - SAFESCHOOLS"

Table 4. Damage factors: 4-story RC dual regularly infilled - PGA: 0.2g.

Model	Damage index	Estimated damage	Damage factor
Fixed (Rock)	Kappos et al. (2006)	$0.26 * 0.0 + 0.51 * 5.0 + 0.16 * 20.0 + 0.04 * 45.0 + 0.03 * 80.0$	10.17%
NL+SSI (D180)	Kappos et al. (2006)	$0.01 * 0.0 + 0.50 * 5.0 + 0.27 * 20.0 + 0.16 * 45.0 + 0.06 * 80.0$	19.74%
Fixed (Rock)	Bal et al. (2008)	$0.26 * 0.0 + 0.51 * 16.0 + 0.16 * 33.0 + 0.04 * 105.0 + 0.03 * 104.0$	21.11%
NL+SSI (D180)	Bal et al. (2006)	$0.01 * 0.0 + 0.50 * 16.0 + 0.27 * 33.0 + 0.16 * 105.0 + 0.06 * 104.0$	39.79%

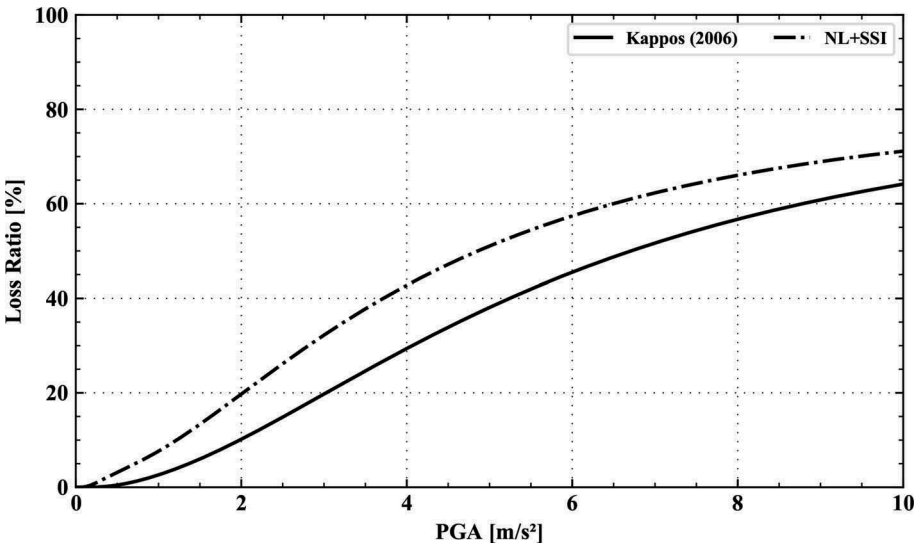

Figure 4. Loss curves for a (i) fixed-base on rock and (ii) flexible-base on soft clay (D180) 4-story dual, regularly infilled building, in the range of 0.0-10.0 m/s^2.

(MIS5030314) which is funded by the Operational Programme "Competitiveness, Entrepreneurship and Innovation" (NSRF 2014-2020) and co-financed by Greece and the European Union (European Regional Development Fund).

REFERENCES

Bal, I.E., Crowley, H. & Pinho, R. 2008. Detail assessment of structural characteristics of Turkish RC buildings stock for loss assessment models. *Soil Dynamics and Earthquake Engineering* 28: 914-932.

Chang, G. & Mander, J. 1994. Seismic energy based fatigue damage analysis of bridge columns: Part I Evaluation of seismic capacity. *NCEER Technical Report* 94-0006.

Crowley, H., Pinho, R. & Bommer, J.J. 2004. A probabilistic displacement-based vulnerability assessment procedure for earthquake loss estimation. *Bulletin of Earthquake Engineering* 2:173-219.

DAyala D., Meslem A., Vamvatsikos D., Porter K., Rossetto T., Crowley H., & Silva V. 2013. Guidelines for Analytical Vulnerability Assessment - Low/Mid-Rise. *GEM Technical Report* 08, 162.

Ghobarah, A. 2004. On Drift Limits Associated with Different Damage Levels. *International Workshop on Performance-Based Seismic Design*. Ontario, Canada.

Kappos, A., Panagopoulos, G., Panagiotopoulos, C. & Penelis, G. 2006. A hybrid method for the vulnerability assessment of R/C and URM buildings. *Bulletin of Earthquake Engineering* 4 (4): 391-413.

Karsan, I. & Jirsa, J. 1969. Behavior of concrete under compressive loadings. *Journal of the Structural Division* ASCE, 95: 2535-2563.

Kent, D.C. & Park, R. 1971. Inelastic behavior of reinforced concrete members with cyclic loading. *Bulletin of the New Zealand Society for Earthquake Engineering* 4(1): 108-125.

Lysmer, J. & Kuhlemeyer, A.M. 1969. Finite dynamic model for infinite media. *Journal of the Engineering Mechanics Division* ASCE, 95: 859-877.

Mazzoni, S., McKenna, F., Scott, M.H. & Fenves, G.L. 2009. Open System for Earthquake Engineering Simulation User Command-Language Manual. Pacific Earthquake Engineering Research Center, Berkeley, USA.

Mylonakis, G., Nikolaou, S. & Gazetas, G. 2006. Footings under seismic loading: Analysis and design issues with emphasis on bridge foundations. *Soil Dynamics and Earthquake Engineering* 26: 824853.

National Institute of Building Sciences 2004. Direct physical damage General building stock. HAZUS-MH Technical manual: Chapter 5. Federal Emergency Management Agency, Washington DC.

Pais, A. & Kausel, E. 1988. Approximate formulas for dynamic stiffnesses of rigid foundations. *Soil Dynamics and Earthquake Engineering* 7(4): 213-227.

Petridis, C. & Pitilakis, D. 2018. Soil-structure interaction effect on earthquake vulnerability assessment of moment resisting frames: the role of the structure. Proc. 16th European Conference on Earthquake Engineering, Thessaloniki, Greece.

Pinho, R., Bommer, J.J. & Glaister, S. 2002. A simplified approach to displacement-based earthquake loss estimation analysis. Proc. 12th European Conference on Earthquake Engineering (ECEE), England.

Pitilakis, D. & Petridis, C. 2018. Soil-structure interaction effect on earthquake vulnerability assessment of moment resisting frames: the role of the soil. Proc. 16th European Conference on Earthquake Engineering, Thessaloniki, Greece.

Pitilakis, K., Crowley, H. & Kaynia, A.M. (eds) 2014. SYNER-G: Typology definition and fragility functions for physical elements at seismic risk. Springer: The Netherlands.

Pitilakis, K., Karapetrou, S. & Fotopoulou, S. 2013. Consideration of aging and SSI effects on seismic vulnerability assessment of RC buildings. *Bulletin of Earhquake Engineering* 12: 17551776.

Rajeev, P. & Tesfamariam, S. 2012. Seismic fragilities of non-ductile reinforced concrete frames with consideration of soil structure interaction. *Soil Dynamics and Earthquake Engineering* 40: 78-86.

Raychowdhury, P. 2008. Nonlinear Winkler-based shallow foundation model for performance assessment of seismically loaded structures. PhD Thesis. University of California, San Diego, USA.

Raychowdhury, P. & Hutchinson, T.C. 2009. Performance evaluation of a nonlinear Winkler-based shallow foundation model using centrifuge test results. *Earthquake Engineering and Structural Dynamics* 38(5): 679-698.

Rossetto, T. & Elnashai, A. 2003. Derivation of vulnerability functions for European-type RC structures based on observational data. *Engineering Structures* 25: 1241–1263.

Scott, B.D., Park, R. & Priestley, M.J.N. 1982. Stress-strain behavior of concrete confined by overlapping hoops at low and high strain rates. *Journal of the American Concrete Institute* 79(1): 13-27.

Vamvatsikos, D. & Cornell, C.A. 2002. Incremental dynamic analysis. *Earthquake Engineering & Structural Dynamics* 31(3): 491-514.

Yepes-Estrada, C., Silva, V., Rossetto, T., D'Ayala, D., Ioannou, I., Meslem, A. & Crowley, H. 2016. The global earthquake model physical vulnerability database. *Earthquake Spectra* 32(4): 2567-2585.